



## Theory of electric-field-controlled surface ferromagnetic transition in metals

Igor V. Ovchinnikov\* and Kang L. Wang†

Department of Electrical Engineering, University of California at Los Angeles, Los Angeles, California 90095-1594, USA

(Received 13 December 2008; published 9 January 2009; publisher error corrected 12 January 2009)

It is widely believed that in metals, unlike in the dilute magnetic semiconductors, the control of ferromagnetic ordering by external voltage is hardly achievable. We compare the two types of ferromagnets and show that there is no obvious reason why metals are less preferable for this phenomenon. A similar effect in metals, however, has a different physical picture and should be identified as a voltage-induced surface transition. We study its properties within the theory of the surface critical phenomena and discuss possible difficulties on the way to its experimental realization.

DOI: 10.1103/PhysRevB.79.020402

PACS number(s): 75.70.-i, 85.75.-d, 85.70.-w

The possibility to externally control ferromagnetic ordering will naturally render an entire additional degree of freedom to the functionality of the magnetoelectronics and spintronics devices.<sup>1</sup> Of primary importance is the capacitive manipulation of ferromagnetism. The voltage-controlled ferromagnetic ordering (VCFO) was demonstrated not long ago<sup>2</sup> in the dilute magnetic semiconductors (DMS).<sup>3</sup> The phenomenon was recognized as a controllable variation in the local (bulk) Curie temperature,  $T_C^b$ , in the surface layer, which the electric field penetrates varying the free-carrier concentration,  $\rho$ , and consequently the free-carrier-mediated exchange coupling between the localized spins. For reasonable voltages, the available variation in  $\rho$  and/or  $T_C$  (Ref. 4) is minor, thus making it imperative that the operation temperature of the device,  $T_0$ , be sufficiently close to the transition point,  $\tau = (T_0 - T_C^b)/T_C^b \rightarrow 0$ . The recent challenge for the technological applications of the VCFO in DMS is that  $T_C$ , and consequently  $T_0$ , is much lower than the room temperature,  $T_R$ .

One of the possible ways to achieve the room-temperature VCFO is to switch to the high- $T_C$  metallic ferromagnets. The conventional wisdom, however, puts forward the two following widely accepted arguments against the possibility of the VCFO in metals: (i) due to the high  $\rho$  the voltage-induced variation in  $T_C$  is inconsiderable in metals; (ii) in metals, the injected carriers occupy only an atomic-size surface layer and so should the voltage-induced magnetization. In this Rapid Communication we show that both arguments are actually misconceptions and a similar effect must exist in metals as recently predicted in Ref. 5. Its physical picture, however, is in a sense opposite of the conventional interpretation. The phenomenon should be viewed not as a local *bulk* but as a *surface* transition, which can be isothermally and reversibly turned on and off by the external voltage. We find the conditions for the existence of the VCFO in metals, obtain the dependence of physical quantities on the applied voltage, and discuss complications, together with possible solutions, on the way to its experimental realization.

The density of itinerant carriers in a ferromagnet defines the strength of the exchange coupling and consequently the magnitude of  $T_C$ . The reserve statement is also qualitatively correct: that  $T_C$  is high directly points out on high  $\rho$  no matter what the ferromagnet is—a metal or a DMS. For example, in the assumption that the increase in doping leads to

the corresponding increase in  $\rho$ ,<sup>6</sup> the  $T_C$  of  $\text{Ga}_{1-x}\text{Mn}_x\text{As}$  was predicted<sup>8</sup> to reach  $T_R$  at  $x \approx 0.1$  and  $\rho > 10^{21} \text{ cm}^{-3}$ , which is usually considered a metallic limit for  $\rho$ . Had argument (i) against the VCFO in metals been true, this would make the recent search for the high- $T_C$  DMS meaningless from the room-temperature VCFO realization point of view. Fortunately, argument (i) is not correct. Near the transition, the temperature fluctuations have already “consumed” the initial coupling strength no matter how high the coupling strength and/or  $\rho$  are. The effectiveness of the charging,  $\rho \rightarrow \rho + \Delta\rho$ , is determined by the voltage-induced shift in the *absolute* value of  $T_C$ ,  $\Delta T_C \approx \Delta\rho \partial_\rho T_C$ , not the *relative*  $T_C$  variation,  $\Delta T_C/T_C \propto \Delta\rho/\rho$ , which indeed drops as  $\rho$  rises.<sup>9</sup>

The injected charge is limited solely by the insulator withstanding the voltage, and  $\Delta T_C$  for different materials varies due to the material-specific  $T_C$  sensitivity,  $\partial_\rho T_C$ . DMS and metals have very different (and in a sense opposite) pictures of their ferromagnetic order: the Ruderman-Kittel-Kotsuya-Yosida (RKKY) theory vs. the Stoner theory. The  $T_C$  sensitivities, however, can be compared for the two representatives of the two classes of ferromagnets:  $\text{Ga}_{1-x}\text{Mn}_x\text{As}$  and  $\text{Ni}_x\text{Cu}_{1-x}$ . In  $\text{Ga}_{1-x}\text{Mn}_x\text{As}$ , the exchange-interaction-mediating carriers are introduced by manganese itself. Each Mn atom contributes roughly one hole to the valence band so that  $\rho \propto x$ . The electron density in  $\text{Ni}_x\text{Cu}_{1-x}$  is also linear in the composition as Cu has an extra electron beyond Ni and, on the other hand, Ni and Cu have identical band structures. Thus, the  $T_C$  sensitivity for both materials is approximately given by the slope of the  $T_C^b(x)$  curve:  $\partial_\rho T_C \sim a^3 \partial_x T_C^b$ , with  $a$  being the lattice constant. The  $T_C^b$  curves obtained experimentally for  $\text{Ni}_x\text{Cu}_{1-x}$  (Ref. 10) and by the mean-field studies for  $\text{Ga}_{1-x}\text{Mn}_x\text{As}$  (Ref. 8) are given (to scale) in Fig. 1(a). It is seen that the slopes are of the same order at  $T_R$ . In fact, the truth about the metallic ferromagnetism is somewhere between the Stoner and the RKKY theories. The  $T_C$ -sensitivity in  $\text{Ni}_x\text{Cu}_{1-x}$  will be even higher than the estimate  $a^3 \partial_x T_C^b$  if we adopt the RKKY picture. Indeed, the change of the electron density in the alloy with  $x$  is split between the localized ( $3d$ ) electrons and the itinerant ( $4s+4p$ ) electrons, whereas by the carrier injection one mostly changes the density of the  $T_C$ -defining itinerant electrons. These observations bring us to the conclusion that there is no obvious reason to believe that in general the absolute value of  $T_C$  is more sensible to the charging in high- $T_C$  DMS than in metals.

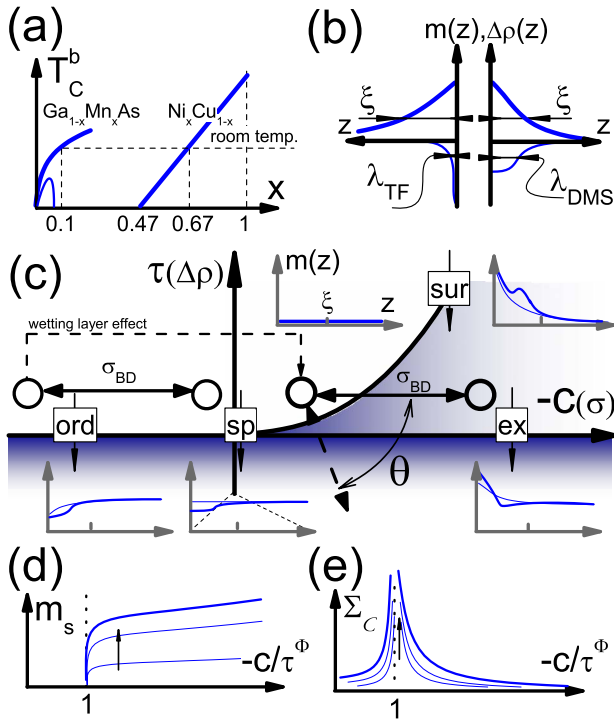


FIG. 1. (Color online) (a)  $T_C^b$  for  $\text{Ga}_{1-x}\text{Mn}_x\text{As}$  from mean-field considerations and  $\text{Ni}_x\text{Cu}_{1-x}$  from experimental studies. The thin line represents  $T_C^b$  of the DMS from Monte Carlo simulations (Ref. 7). (b) Even though the width of the injected charge distribution,  $\Delta\rho(z)$ , (thin lines) is higher in the high- $T_C$  DMS (right side),  $\lambda_{\text{TF}} < \lambda_{\text{DMS}}$ , the magnetization profile,  $m(z)$ , (thick lines) being determined by the spin-spin-correlation length,  $\xi$ , is wider in metals (left side). (c) The phase plane  $(\tau, c)$  of a semi-infinite ferromagnet consists of the three regions: the paramagnetic, the ferromagnetic, and the surface ferromagnetic phases. The corresponding mean-field (thin lines) and RG-corrected (thick lines) magnetization profiles are qualitatively given in the insets. The ordinary (ord), the special (sp), the extraordinary (ex), and the surface (sur) transitions are indicated by the black vertical arrows. With the carrier injection one shifts the metallic surface on the  $c$  scale (double-headed arrows), and at  $\tau \rightarrow +0$  it is possible to turn the surface magnetization on and off if  $c < \sigma_{\text{BD}}$  (see text). The dashed double-headed arrow represents the effect of charging in low- $T_C$  DMS material. The effect of the wetting layer (see text) is also shown. [(d)–(e)] The excess magnetization,  $m_s$ , and the capacitance renormalization function,  $\Sigma_C$ , as functions of  $c$  (and/or of the injected charge,  $\sigma$ ). The arrows indicate the modification of the profiles as  $\tau \rightarrow +0$ .

The spatial behavior of the magnetization does not go beyond the spin-spin-correlation length,  $\xi = \Lambda |\tau|^{-\nu}$ , where  $\nu$  is the critical exponent of the bulk transition ( $\nu \approx 0.63$  for  $d=3$ ,  $n=1$ ) and the cutoff  $\Lambda > a$ . Thus, the width of the voltage-induced surface magnetization is given by the largest of the two lengths:  $\xi$  and the electric-field penetration length. The device operates in the critical region and  $\xi$  is large. In fact,  $\xi$  is limited only by the experimental accuracy with which it is possible to maintain the device at a fixed  $T_0$  stably, and the record  $\xi$  values can go well above 100 nm.

The electric-field penetration length in metals is given by the Thomas-Fermi screening radius,  $\lambda_{\text{TF}} \approx a \ll \xi$ . In doped semiconductors, the electric-field penetration length can be

as high as hundreds of nanometers at low doping (right above the percolation threshold,  $\rho \sim 10^{16} \text{ cm}^{-3}$ ). In the high- $T_C$  DMS case ( $\rho > 10^{21} \text{ cm}^{-3}$ ), however,  $\lambda_{\text{DMS}}$  is given by the Debye screening radius,<sup>11</sup> which upon estimation will not exceed a dozen nanometers. Even though  $\lambda_{\text{DMS}} \gg \lambda_{\text{TF}}$ , it is not as high as the record values of  $\xi$  so that in both metals and high- $T_C$  DMS the width of the magnetization profile is determined by  $\xi$  [see Fig. 1(b)]. The metallic ferromagnetic ordering is “stiffer” ( $\Lambda_{\text{metal}} > \Lambda_{\text{DMS}}$ ) and  $\xi_{\text{metal}} > \xi_{\text{DMS}}$  for equal  $\tau$ . Thus, argument (ii) is also a misconception and the voltage-induced magnetization layer must be wider on a metallic surface.

At the transition, the qualitative reconstruction of the system’s properties happen on a macroscopically large scale. The zero-temperature local picture of the magnetoelectric effect on a surface<sup>12</sup> breaks down at the criticality and by no means applies to the VCFO, which at its very essence is a phase transition. The proper physical description can only be given in terms of the theory of the surface critical phenomena (see, e.g., Refs. 13–16), which is based on the formalism of the Ginzburg-Landau energy functional. At this, the difference between the magnetic properties of the surface and the bulk atoms is accounted for by an additional surface-integral term,  $c \int_S m^2$ , where  $m$  is the spatial density of the magnetization and  $c$  is the surface enhancement. That  $c$  is negative reflects the fact that the surface atomic layer is locally “more” ferromagnetic than the bulk. The effects of the surface-enhanced magnetization<sup>17</sup> and the so-called magnetic “dead” layers<sup>18</sup> can be viewed as direct indications that  $c \leq 0$ , respectively.

The renormalization-group (RG) flow of a near-critical semi-infinite ferromagnet is governed by the Wilson’s fixed point<sup>19</sup> on the *coupling-constant- $\tau$*  plane. The enhancement, however, is also a relevant field<sup>16</sup> with the cross scaling  $c \propto \tau^\Phi$ , where  $\Phi$  is the so-called crossover exponent ( $\Phi \approx 0.58$  for  $d=3$  and  $n=1$ ). Accordingly, the long-wavelength properties of the system are uniquely defined by the position on the  $\tau$ - $c$  phase plane, which consists of the three distinct regions:<sup>15</sup> the paramagnetic phase, the ferromagnetic phase, and the surface ferromagnetic phase in which the magnetization exists only at the surface [see Fig. 1(c)]. Depending on the value of  $c$ , the ferromagnetic ordering of the bulk at  $\tau = 0$  is referred to as the ordinary ( $c > 0$ ), the special ( $c = 0$ ), and the extraordinary ( $c < 0$ ) transitions. In addition, for  $c < 0$  and  $\tau > 0$  there also exists the surface transition from the paramagnetic to the surface ferromagnetic phases. The surface transition has a separate Curie temperature,  $T_C^s \geq T_C^b$ ,  $\tau_s = (T_C^s - T_C^b)/T_C^b$ , which is determined up to an interface-specific factor by the cross scaling,  $\tau_s = (-c)^{1/\Phi}$ .

In metals, the injected charge resides exactly in the surface atoms, which determine the surface enhancement. To a first approximation, the charging can be viewed as a linear variation,  $c \rightarrow c + v\sigma$ , with  $\sigma = \int dz \Delta\rho(z)$  being the injected surface charge and  $v$  being another interface-specific parameter. On the phase plane, charging a metal looks like the controllable shift along the  $c$  axis. As long as  $\lambda_{\text{DMS}} \ll \xi$ , the same picture of the VCFO applies to the high- $T_C$  DMS. In case the electric-field penetration length is comparable with  $\xi$ , the case which is most likely realized in the low- $T_C$  DMS, the surface electron system “sees” the VCFO as a partly bulk

and partly surface transition. On the phase plane, the charging can be effectively viewed as the shift in both axes at the angle  $\theta = \tan^{-1} \lambda_{\text{DMS}} / \xi$ . The conventional picture of the VCFO as of a local bulk transition, i.e., of shifting the system along the  $\tau$  axis ( $\theta \rightarrow \pi/2$ ), is recovered only in the hypothetical situation when  $\xi \ll \lambda_{\text{DMS}}$ .

Phase transitions reveal themselves through singular contributions to various physical quantities,  $Q^{(\text{sing})}$ . Typically, one is interested in the  $\tau$  dependence of  $Q^{(\text{sing})}$ , treating  $c$  as a fixed parameter of the system. The situation is opposite for the VCFO, where  $\tau$  is fixed and it is  $c$ , which is variable by the applied voltage. The voltage dependence of  $Q^{(\text{sing})}$  can be derived from the scaling hypothesis,<sup>14</sup> which implies the following:

$$Q^{(\text{sing})}(\tau, c) = \tau^\Gamma f_Q(c/\tau^\Phi), \quad (1)$$

with  $f_Q(x)$  being a smooth function with the power-law singularities at the transition points,  $x = \pm\infty, -1$ . The singularities can be obtained by the requirement that at different transitions ( $x=0, -1, \pm\infty$ ) Eq. (1) should provide the corresponding  $\tau$  exponents, which are known for the ordinary, the special, and the surface transitions:  $Q^{(\text{sing})} \propto \tau^{\gamma_Q^{\text{sp,ord}}}$ ,  $\tau \rightarrow 0$  for  $c=0, +\infty$ , respectively, and  $Q^{(\text{sing})} \propto |\tau - \tau_s|^{\gamma_Q^{\text{sur}}}$ ,  $\tau \rightarrow \tau_s$ .

The extraordinary transition case ( $c \rightarrow -\infty$ ) is more subtle.<sup>13-15</sup> The source of the difficulty in the theoretical studies is in the weakness of the singularities in the presence of already existing surface magnetization. We appeal to a heuristic argument that the extraordinary and ordinary transitions can be viewed as two close points on the opposite sides of the point  $c=\infty$  on the Reimann loop. From this perspective,  $c=\infty$  is a transition point separating the paramagnetic and the surface ferromagnetic phases. As such, the exponents of  $Q^{(\text{sing})}$  should be the same  $\gamma_Q^{\text{ex}} = \gamma_Q^{\text{ord}}$ . This is at least true for  $\alpha_s$  and  $\beta_s$  exponents,<sup>13</sup> which are of specific interest to us (see below). With this assumption we arrive at  $\Gamma_Q = \gamma_Q^{\text{sp}}$ ,  $f_Q(x) \propto |x+1|^{\gamma_Q^{\text{sur}}}$  as  $x \rightarrow -1$ , and  $f_Q(x) \propto |x|^{(\gamma_Q^{\text{sp}} - \gamma_Q^{\text{ord}})/\Phi}$  as  $x \rightarrow \pm\infty$ ; and consequently,

$$Q^{(\text{sing})} = \begin{cases} \tau^{\gamma_Q^{\text{sur}}} |\tau^\Phi + c|^{\gamma_Q^{\text{sur}}} \Xi_Q, & |\tau^\Phi + c| < \tau^\Phi \\ \tau^{\gamma_Q^{\text{ord}}} |c|^{\gamma_Q^{\text{ord}}} \Xi_Q, & |c| \gg \tau^\Phi, \end{cases} \quad (2)$$

where  $\gamma_{Q,\tau}^{\text{sur}} = \gamma_Q^{\text{sp}} - \Phi \gamma_Q^{\text{sur}}$ ,  $\gamma_{Q,c}^{\text{sur}} = \gamma_Q^{\text{sur}}$ ,  $\gamma_{Q,\tau}^{\text{ord}} = \gamma_Q^{\text{ord}}$ ,  $\gamma_{Q,c}^{\text{ord}} = (\gamma_Q^{\text{ord}} - \gamma_Q^{\text{ord}})/\Phi$ , and  $\Xi_Q$  is a decently behaving crossover function, which can contain weak logarithmic corrections to the explicit power-law singularities.

The two physical quantities directly measurable experimentally are our primary interest. The first one is the excess magnetization per surface area, which is straightforwardly obtainable through, e.g., superconducting quantum interference device (SQUID) measurements. The other quantity is the excess surface energy (per surface area),  $f_s$ . The transition should contribute to the overall surface capacitance as  $C^{-1} = C_0^{-1} - \Sigma_c(c)$ , where  $C_0$  is the electrostatic capacitance of the device geometry and  $\Sigma_c(c) = -2\partial^2 f_s / \partial c^2$ . This singular contribution should be measurable by the conventional elec-

tronics means, e.g., by the differential capacitance measurements. In terms of Eq. (2):  $\gamma_{\Sigma_c, \tau}^{\text{sur,ord}} = \gamma_{f_s, \tau}^{\text{sur,ord}}$  and  $\gamma_{\Sigma_c, c}^{\text{sur,ord}} = \gamma_{f_s, c}^{\text{sur,ord}} - 2$ .

The exponents for  $m_s$  and  $f_s$  are known in the literature as  $\gamma_{m_s} = \beta_s$  and  $\gamma_{f_s} = 2 - \alpha_s$ . At the surface transition, the bulk is not critical and all the exponents are those of the  $(d-1)$ -dimensional bulk transition:  $\beta_s^{\text{sur}} = \beta_b^{(d-1)}$ ,  $\alpha_s^{\text{sur}} = \alpha_b^{(d-1)}$ . The surface transition is essentially 2D and it should exist<sup>20</sup> in the presence of even vanishingly small perpendicular anisotropy (see below). The assumption that at the ordinary and the special transitions (at which the surface is not critical solely) there is only one relevant scale,  $\xi$ , or that  $f_s \propto (1/\xi)^{d-1}$ , leads to the conclusion that  $\alpha_s^{\text{sp,ord}} = \alpha_b^{(d)} + \nu^{(d)}$  and  $\beta_s^{\text{sp,ord}} = \beta_b^{(d)} - \nu^{(d)}$ . The two basic scaling laws  $\beta_b^{(d)} = \nu^{(d)}(d-2 + \eta^{(d)})/2$  and  $\alpha_b^{(d)} = 2 - d\nu^{(d)}$  relate the exponents to the two principle bulk exponents  $\nu$  and  $\eta$ , which are known for different dimensions and different numbers of the components of the order parameter,  $n$ .

The vicinity of the surface (and/or the flat geometry of the device) should impose a strong perpendicular easy-axis anisotropy, as is known from the studies of thin magnetic films.<sup>21</sup> Therefore, among different choices of  $n$  for the surface transition,  $n=1$  is probably the most pertinent one. At last, up to the second order in  $\epsilon = 4-d$  (Ref. 19) we have ( $d=3, n=1$ ):  $\gamma_{m_s, \tau}^{\text{sur}} = -0.33$ ,  $\gamma_{m_s, c}^{\text{sur}} = 0.031$ ,  $\gamma_{m_s, \tau}^{\text{ord}} = -0.31$ ,  $\gamma_{m_s, c}^{\text{ord}} = 0$  and  $\gamma_{\Sigma_c, \tau}^{\text{sur}} = 0.11$ ,  $\gamma_{\Sigma_c, c}^{\text{sur}} = -0.32$ ,  $\gamma_{\Sigma_c, \tau}^{\text{ord}} = 1.25$ ,  $\gamma_{\Sigma_c, c}^{\text{ord}} = -2$ . That the power-law singularity vanishes for  $m_s$  at high  $c$ 's ( $\gamma_{m_s, c}^{\text{ord}} = 0$ ) implies that the logarithmic singularity takes over and Eq. (2) should be corrected for  $m_s$  as  $\propto \tau^{\gamma_{m_s, \tau}^{\text{ord}}} \ln(|c|/\tau^\Phi)$ , for  $|c| \gg \tau^\Phi$ . The resulting curves for  $m_s$  and  $\Sigma_c$  are given in Figs. 1(d) and 1(e).

Numerical estimations can be obtained from mean-field considerations. At this, the material-specific Ginzburg-Landau functional parameters should be acquired from some additional physical arguments. In Ref. 5, this was done for  $\text{Ni}_x\text{Cu}_{1-x}$  in the framework of the orbital-free spin-density-functional theory. The rise of  $T_C^s$  (at initial  $c=0$ ) due to the charge injection, withstandable by  $\text{SiO}_2$ , was found to be on order of dozens kelvins. In a similar manner one can obtain the following estimates for the crossover functions in Eq. (2):  $\Xi_{m_s} \approx 10^{13-14} \mu_B \text{ cm}^{-2}$  and  $\Xi_{\Sigma_c} \approx 10^{-5-6} \text{ J cm}^{-2}$ , which lie within the sensitivity of modern measuring tools. In fact, due to the small stiffness coefficient, the model proposed in Ref. 5 underestimates the magnetic response and overestimates the voltage variability of  $T_C^s$ . The possibly low  $T_C^s$  variability, however, can be experimentally compensated by switching to the ferroelectric insulators in which the available surface charge is on the order of magnitude higher than in  $\text{SiO}_2$ .

If from the theoretical point of view a rather close look at the VCFO in metals can be taken with relative ease by building on the previous work on the surface critical phenomena, the experimental observation of this effect may claim some effort and diligence. As is seen from Figs. 1(d) and 1(e) the strongest ferromagnetic response should be at the tricritical point ( $c, \tau \rightarrow 0$ ). Tuning the interface to the tricritical point on each of the two phase-plane axes is a matter of two separate experimental challenges.

$T_C$  of most metallic ferromagnets used recently is usually much higher than  $T_R$ . This is the reason why the room-temperature metallic ferromagnetism was controllable so far only in ultrathin films.<sup>22</sup> In order to bring the VCFO in metals to 100 nm scale it is necessary to tune  $T_C$  close to  $T_R$ . This is achievable by the use of ferromagnetic alloys with the composition-dependent  $T_C$ ; e.g., for  $\text{Ni}_x\text{Cu}_{1-x}$ ,  $T_C^b = T_R$  at  $x=0.67$ .

As for tuning the system on the  $c$  axis, it is clear from Fig. 1(c) that due to the limitation on the charging, imposed by the insulating material breakdown,  $|\sigma| < \sigma_{\text{BD}}$ , the VCFO is only possible if  $c < \sigma_{\text{BD}}$ . Due to such surface effects as misfit, hybridization of the electron levels, etc., the surface enhancement is specific not only to the ferromagnet itself but also to the contact material. It is possible that none of the available *ferromagnet-insulator* pairs will satisfy the above requirement on  $c$ . The solution can be found in what could be called a “wetting” layer—a monolayer of a different material between the contacts. It is likely that an intrinsically extraordinary ferromagnet such as the lanthanides Gd (Ref. 23) and Tb (Ref. 24) must be used for a wetting layer.

Concluding our discussion, we showed that the effect of the high-temperature voltage-controlled ferromagnetism does not favor only the high- $T_C$  DMS and should exist in metallic ferromagnets as well. We clarified the physical picture of this phenomenon in metals and high- $T_C$  DMS, identifying it with the voltage-controlled transition on a surface, which is close enough to the tricritical point on the *temperature-surface enhancement* phase plane. Within the theory of the surface critical phenomena we found the “voltage” critical exponents for the excess surface magnetization and surface energy. We proposed that the required proximity of the tricritical point can be achieved by using ferromagnetic alloys with  $T_C$  tunable by the composition and by means of a wetting monolayer of a different material between the insulator and the ferromagnet.

The work was supported in part by Western Institute of Nanoelectronics (WIN) funded by the NRI, Center on Functional Engineered NanoArchitectonics (FENA) funded by FCRP, and ARO MURI.

\*iovchinnikov@ucla.edu

†wang@ee.ucla.edu

<sup>1</sup>S. A. Wolf, D. D. Awschalom, R. A. Buhrman, J. M. Daughton, S. von Molnar, M. L. Roukes, A. Y. Chtchelkanova, and D. M. Treger, *Science* **294**, 1488 (2001).

<sup>2</sup>H. Ohno, D. Chiba, F. Matsukura, T. Omiya, E. Abe, T. Dietl, Y. Ohno, and K. H. Ohtani, *Nature (London)* **408**, 944 (2000).

<sup>3</sup>Y. D. Park, A. T. Hanbicki, S. C. Erwin, C. S. Hellberg, J. M. Sullivan, J. E. Mattson, T. F. Ambrose, A. Wilson, G. Spanos, and B. T. Jonker, *Science* **295**, 651 (2002); I. Žutić, J. Fabian, and S. Das Sarma, *Rev. Mod. Phys.* **76**, 323 (2004); A. H. MacDonald, P. Schiffer, and N. Samarth, *Nature Mater.* **4**, 195 (2005); T. Jungwirth, J. Sinova, J. Masek, J. Kucera, and A. H. MacDonald, *Rev. Mod. Phys.* **78**, 809 (2006).

<sup>4</sup>We use  $T_C$  to refer to the Curie temperature in general, whereas  $T_C^b$  and  $T_C^s$  specify the bulk and the surface  $T_C$ 's.

<sup>5</sup>I. V. Ovchinnikov and K. L. Wang, *Phys. Rev. B* **78**, 012405 (2008).

<sup>6</sup>The recent Monte Carlo studies (Ref. 7) unveiled that  $\rho$  drops in DMS at higher  $x$ . Thus, since  $\rho$  determines  $T_C$ ,  $T_C$  in DMS does not probably reach  $T_R$  at all. Here, we assume, giving credit to DMS, that the increase in  $x$  is accompanied by the corresponding increase in  $\rho$  and that high- $T_C$  case in DMS is indeed realizable.

<sup>7</sup>G. Alvarez, M. Mayr, and E. Dagotto, *Phys. Rev. Lett.* **89**, 277202 (2002); F. Popescu, Y. Yildirim, G. Alvarez, A. Moreo, and E. Dagotto, *Phys. Rev. B* **73**, 075206 (2006).

<sup>8</sup>T. Dietl, H. Ohno, F. Matsukura, J. Cibert, and D. Ferrand, *Science* **287**, 1019 (2000); T. Dietl, H. Ohno, and F. Matsukura, *Phys. Rev. B* **63**, 195205 (2001); A. Chattopadhyay, S. Das Sarma, and A. J. Millis, *Phys. Rev. Lett.* **87**, 227202 (2001).

<sup>9</sup>As will be clarified later, it is the surface charge density, which is the appropriate controlling variable. The conventional picture of the  $T_C$  variation by varying  $\rho$  suffices as an argument for the next paragraph.

<sup>10</sup>S. A. Ahern, M. J. Martin, and W. Sucksmith, *Proc. R. Soc. Lond.* **248**, 145 (1958).

<sup>11</sup>This is another credit to the high- $T_C$  DMS. Within the widely accepted RKKY picture of the DMS, the itinerant carriers form a statistically degenerate Fermi liquid and the screening length is also defined by the Thomas-Fermi radius.

<sup>12</sup>C. S. Duan, J. P. Velev, R. F. Sabirianov, Z. Q. Zhu, J. H. Chu, S. S. Jaswal, and E. Y. Tsymlal, *Phys. Rev. Lett.* **101**, 137201 (2008).

<sup>13</sup>H. W. Diehl, in *Phase Transitions and Critical Phenomena*, edited by C. Domb and J. L. Lebowitz (Academic, London, 1986), Vol. 10; K. Binder and P. C. Hohenberg, *Phys. Rev. B* **6**, 3461 (1972); Y. Okabe and K. Ohno, *ibid.* **30**, 6573 (1984).

<sup>14</sup>A. J. Bray and M. A. Moore, *J. Phys. A* **10**, 1927 (1977).

<sup>15</sup>T. C. Lubensky and M. H. Ruben, *Phys. Rev. Lett.* **31**, 1469 (1973); *Phys. Rev. B* **12**, 3885 (1975).

<sup>16</sup>H. W. Diehl, G. Gompper, and W. Speth, *Phys. Rev. B* **31**, 5841 (1985).

<sup>17</sup>C. A. Queiroz and W. Figueiredo, *Phys. Rev. B* **40**, 4967 (1989); T. Komesu, C. Waldfried, and P. A. Dowben, *Phys. Lett. A* **256**, 81 (1999).

<sup>18</sup>S. K. Kim, J. R. Jeong, J. B. Kortright, and S. C. Shin, *Phys. Rev. B* **64**, 052406 (2001).

<sup>19</sup>K. G. Wilson, *Phys. Rev. Lett.* **28**, 548 (1972).

<sup>20</sup>M. Bander and D. L. Mills, *Phys. Rev. B* **38**, 12015 (1998).

<sup>21</sup>C. A. F. Vaz, J. A. C. Bland, and G. Lauthoff, *Rep. Prog. Phys.* **71**, 056501 (2008); M. T. Johnson, P. J. H. Bloemen, F. J. A. den Broeder, and J. J. de Vries, *ibid.* **59**, 1409 (1996).

<sup>22</sup>M. Weisheit, S. Fahler, A. Marty, Y. Souche, C. Poinsignon, and D. Givord, *Science* **315**, 349 (2007).

<sup>23</sup>D. Weller, S. F. Alvarado, W. Gudat, K. Schroder, and M. Campagna, *Phys. Rev. Lett.* **54**, 1555 (1985).

<sup>24</sup>C. Rau and C. Jin, *J. Appl. Phys.* **63**, 3667 (1988).